ACS SENSORS

pubs.acs.org/acssensors

Article

Genetic Encoding of Fluorinated Analogues of Phenylalanine for ^{19}F NMR Spectroscopy: Detection of Conformational Heterogeneity in Flaviviral NS2B-NS3 Proteases

Haocheng Qianzhu,[§] Yi Jiun Tan,[§] Elwy H. Abdelkader, Thomas Huber,* and Gottfried Otting*

Cite This: *ACS Sens.* 2025, 10, 3152−3161

Read Online

ACCESS | Metrics & More | Article Recommendations | Supporting Information

ABSTRACT: Substituting a single hydrogen atom in a protein by fluorine provides a probe for site-specific sensing by ^{19}F nuclear magnetic resonance (NMR) spectroscopy with minimal impact on the properties of the protein. Genetic encoding systems are presented for five different fluorinated analogues of phenylalanine: 2-, 3-, 4-fluorophenylalanine, 2,6-difluorophenylalanine, and 3,5-difluorophenylalanine. The systems allow the installation of each of these amino acids with high fidelity during in vivo bacterial protein synthesis in response to an amber stop codon. The respective target proteins are obtained in high yield. At the site of Phe116 in different constructs of the dengue virus and Zika virus NS2B-NS3 proteases, the fluorinated phenylalanine analogues reveal evidence of significant conformational heterogeneity in ^{19}F NMR spectra and demonstrate conformational dynamics. The availability of different ^{19}F NMR probes allows discriminating between impacts arising from the fluorine atoms and the properties intrinsic to the protein.

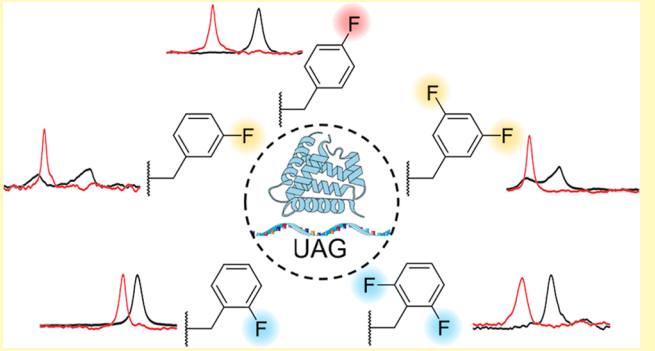

KEYWORDS: *aminoacyl-tRNA synthetase, dengue virus protease, difluorophenylalanine, fluorophenylalanine, ^{19}F NMR spectroscopy, NS2B-NS3 protease, Zika virus protease*

Downloaded via AUSTRALIAN NATL UNIV on May 4, 2026 at 00:40:28 (UTC).
See https://pubs.acs.org/sharingguidelines for options on how to legitimately share published articles.

Proteins produced with phenylalanine (Phe) analogues containing hydrogen-to-fluorine substitutions in the phenyl ring have long been recognized to display exceptionally large chemical shift dispersions in ^{19}F nuclear magnetic resonance (NMR) spectra,[1] which facilitates the detection of minor conformational species.[2] In the case of global substitutions of Phe to fluorinated phenylalanine analogues, however, the structure and function of the protein may be compromised by the multiple fluorine atoms. As a CF group is only little larger than the CH group it replaces, the effects arising from global substitution of amino acids by singly fluorinated analogues tend to be small,[3−6] but the cumulative effects from multiple CH−CF substitutions can nonetheless become noticeable.[7,8] Dilution of the fluorinated amino acid with its canonical parent reduces these potential structural perturbations but also severely compromises sensitivity and renders the samples chemically heterogeneous.[9] In addition, proteins of high molecular weight display broad ^{19}F NMR resonances due to ^{19}F relaxation governed by pronounced chemical shift anisotropy (CSA) relaxation,[10] which makes it difficult to assign the ^{19}F NMR signals by techniques other than site-directed mutagenesis.[11]

To minimize any perturbation created by the hydrogen-to-fluorine substitution and resolve the assignment problem, the ideal scenario is the substitution of a single Phe residue in the protein by a fluorinated analogue, amounting to a protein where a single hydrogen atom is replaced by a fluorine atom. This can be accomplished by genetic encoding of the noncanonical amino acid (ncAA). It requires an orthogonal translation system (OTS), where an aminoacyl-tRNA synthetase (RS) specifically recognizes the target ncAA and covalently attaches it to a suppressor-tRNA, which is orthogonal to the native tRNAs and installs the ncAA in response to an amber stop codon. The subtle chemical difference between fluorinated and canonical phenylalanine makes genetic encoding challenging because the native *Escherichia coli* phenylalanyl-tRNA synthetase, while preferring canonical phenylalanine, also functions with fluorophenylalanines. Installation of fluorinated phenylalanine with the help of chemically aminoacylated suppressor-tRNA has been demonstrated but only very small amounts of fluorine-modified protein were obtained.[12]

Received: February 6, 2025
Revised: March 18, 2025
Accepted: March 26, 2025
Published: April 1, 2025

ACS Publications

© 2025 American Chemical Society

https://doi.org/10.1021/acssensors.5c00432
ACS Sens. 2025, 10, 3152−3161

In an early attempt of genetic encoding of 4-fluorophenylalanine (4F-Phe) in vivo, Furter deployed a yeast $tRNA_{CUA}^{Phe}$/phenylalanyl-tRNA synthetase pair in an analogue-resistant *E. coli* strain,[13] but the system only incompletely discriminated between Phe and 4F-Phe, yielding nonuniform protein preparations. A polyspecific mutant of *Methanocaldococcus jannaschii* tyrosyl-tRNA synthetase was subsequently shown to install 4F-Phe in response to an amber stop codon but the protein yields were low.[14] More recently, mutants of pyrrolysyl-tRNA synthetases have been explored for their capacity to genetically encode other fluorinated Phe analogues. For example, a polyspecific mutant of *Methanosarcina mazei* pyrrolysyl-tRNA synthetase (*Mm*PylRS) was found to recognize 3F-Phe, albeit with an efficiency insufficient for outcompeting the natural *E. coli* phenylalanyl-tRNA synthetase, resulting in a significant background of 3F-Phe replacing Phe.[15] Another polyspecific *Mm*PylRS mutant was found to recognize 2-fluorophenylalanine (2F-Phe) and 2,6-difluorophenylalanine (2,6diF-Phe) with modest efficiency.[16] Further mutagenesis delivered a mutant capable of aminoacylating $tRNA_{CUA}^{Pyl}$ with 3,5-difluorophenylalanine (3,5diF-Phe),[17] but protein yields were not reported. Finally, two different polyspecific *Methanosarcina barkeri* pyrrolysyl-tRNA synthetase (*Mb*PylRS) mutants have been shown to install 2,6diF-Phe, 3,5diF-Phe, and 2F-Phe as well as a number of more highly fluorinated Phe analogues in superfolder green fluorescent protein (sfGFP) in *E. coli* and HEK 293T cells, with best efficiency for the more highly fluorinated amino acids.[18] The protein expression yields in *E. coli* were not reported. In HEK cells, the most robust expression achieved was 34 μg of target protein with pentafluoro-phenylalanine per gram of cell pellet.

In previous work, OTSs based on the pyrrolysyl-tRNA synthetase of the methanogenic archaeon ISO4-G1 (G1PylRS) proved to enable the incorporation of 4-, 5-, 6-, and 7-fluorotryptophans and other ncAAs with high yield and fidelity.[19−23] Phenylalanine occurs about 3-fold more frequently in the proteome than tryptophan,[24] correspondingly raising the utility of OTSs that encode fluorinated phenylalanine analogues. The generally modest protein yields of the *Mm*PylRS and *Mb*PylRS systems for aromatic fluorinated amino acids, however, along with persistent difficulties of discriminating between natural Phe and singly fluorinated Phe, present an ongoing bottleneck. This prompted us to explore a G1PylRS library for mutant RS enzymes that achieve the genetic encoding of 2F-Phe, 3F-Phe, 4F-Phe, 2,6diF-Phe, and 3,5diF-Phe (Figure 1a−e) in high yield and purity. We demonstrate the performance of the OTSs discovered by site-selectively installing all these different versions of fluoro- and difluorophenylalanines into the NS2B-NS3 proteases (NS2B-NS3pro) of the dengue virus serotype 2 and the Zika virus.

The flaviviral NS2B-NS3 proteases are established drug targets, for which the development of medically viable small molecule inhibitors has proven difficult.[25] The wild-type proteases are composed of two polypeptide chains, NS2 and NS3, both of which are essential for protease activity, and the C-terminal part of NS2B, in the following referred to as NS2Bc, is only loosely associated with NS3, forming open and closed conformations. Proteolytic activity depends on the closed conformation where NS2Bc forms a β-hairpin that completes the substrate binding site. Multiple crystal structures of the NS2B-NS3 proteases have shown that NS2Bc adopts a closed conformation in the presence of an active site inhibitor

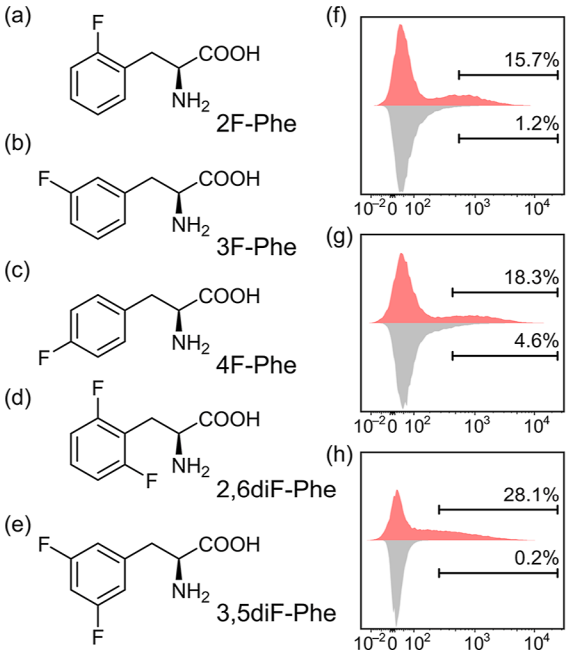

Figure 1. Chemical structures of the fluorinated phenylalanine analogues for which genetic encoding systems were developed in the present work: (a) 2-fluorophenylalanine (2F-Phe), (b) 3-fluorophenylalanine (3F-Phe), (c) 4-fluorophenylalanine (4F-Phe), (d) 2,6-difluorophenylalanine (2,6diF-Phe), (e) 3,5-difluorophenylalanine (3,5diF-Phe) and histograms from the final rounds of fluorescence-activated cell sorting (FACS) selection to identify G1PylRS enzymes active toward (f) 2F-Phe, (g) 4F-Phe, and (h) 2,3,4,5,6-pentafluorophenylalanine (F_5-Phe). The horizontal axis reports the red fluorescence intensity from expression of the mCherry red fluorescent protein (RFP) gene, which is interrupted by an amber stop codon so that red fluorescence indicates successful aminoacylation of the G1 suppressor-tRNA. The vertical axis represents the cell count, with the RFP fluorescence of cells grown with ncAA plotted in the positive direction (red) and the RFP fluorescence measured without ncAA plotted in the negative direction (gray). The presence of many more cells with intense red fluorescence in the presence versus absence of the ncAA indicates the presence of ncAA-specific RS enzymes in the gene pool.

(Figure 2). In the absence of a ligand, however, NS2Bc is usually dislocated from the substrate binding site, forming an open conformation and often leading to unobservable electron density in the X-ray structures (Table S1).[26−32] In contrast, the N-terminal segment of NS2B is always observed, being an integral part of one of the β-barrels of NS3pro regardless of the presence or absence of inhibitors (Figure 2a,b). These data suggest that the open conformation of the NS2B-NS3 proteases is a straightforward target for inhibitors. NMR spectroscopy data measured in solution, however, have provided a more nuanced picture of the state of NS2Bc.

NMR experiments performed of the NS2B-NS3 proteases from dengue (serotype 2) and Zika virus indicated that the equilibrium between open and closed conformations depends on the construct used and the solution conditions. To ensure equimolar ratios of NS2B and NS3pro and maintain the long term activity of the proteases, constructs of the NS2B-NS3 proteases are commonly produced with the peptide Gly_4−Ser−Gly_4 covalently linking the C-terminus of NS2B with the N-terminus of NS3pro.[33] We refer to these NS2B-NS3 protease constructs as gDENV and gZika. Alternatively, the link can contain a recognition sequence for enzymatic self-cleavage. We

https://doi.org/10.1021/acssensors.5c00432
ACS Sens. 2025, 10, 3152−3161

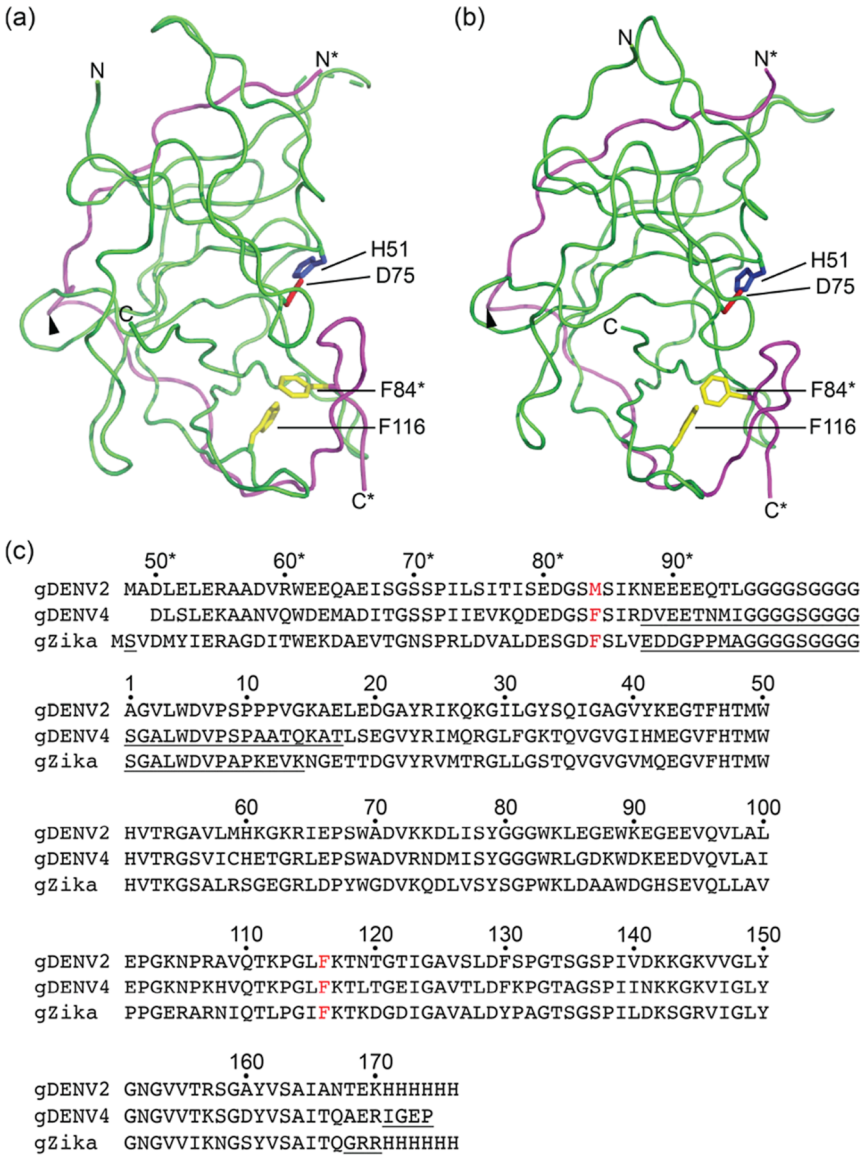

Figure 2. Dengue and Zika virus NS2B-NS3 proteases. In this figure, constructs from dengue virus serotypes 2 and 4 are labeled gDENV2 and gDENV4, respectively. Residue numbers in NS2B are labeled with a star. (a) Structure of gDENV4 in the closed conformation (PDB ID 5YVU).[32] The backbone of NS3pro and NS2B is shown in green and magenta, respectively. The binding site of BPTI and inhibitor **1** (Figure S1) is marked by the active site residues H51 and D75 of the catalytic triad in NS3pro. The first and last residues of NS2B detected in the crystal structures and the first and last residues of NS3pro are identified. The side chains of F84* (yellow), F116 (yellow), H51 (blue), and D75 (red) are highlighted. NS2B residues N-terminal of E63*, identified by an arrow, are structurally conserved in the open and closed conformations. (b) Structure of gZika in the closed conformation (PDB ID 5LC0).[29] The full structure includes a peptide inhibitor (not shown) at the active site. Color coding and labeling as in (a). (c) Amino acid sequence alignment of the gDENV2 and gZika constructs used in the present work. Residues 84* in NS2B and 116 in NS3pro, which are within 4 Å of each other in the crystal structure, are highlighted in red. The amino acid sequence of gDENV4 of the crystal structure 5YVU is shown for comparison. Underlining identifies residues for which no electron density was observed in the crystal structures of 5YVU and 5LC0 despite their presence in the amino acid sequence. In the linked constructs gDENV and gZika, NS2B and NS3pro are connected via the Gly_4−Ser−Gly_4 peptide. The unlinked constructs eDENV2 and eZika were obtained by substituting the Gly_4−Ser−Gly_4 linker by the peptide segments EVKKQR and VKTGRK, which constitute recognition sites for proteolytic cleavage by the respective proteases.

refer to these constructs as unlinked and name the respective protease constructs eDENV and eZika (Figure 2c). Previous NMR experiments of eDENV and gDENV had indicated the closed conformation both in the presence and absence of inhibitors.[34−36]

When the gZika construct was investigated by NMR spectroscopy, a closed conformation was found in the presence of a covalently binding boronate inhibitor.[37] In the absence of inhibitors, some of the backbone amides attributed to NS2Bc displayed slowly relaxing NMR signals indicative of greatly increased mobility as expected for the open conformation.

An unlinked construct of the Zika virus NS2B-NS3 protease reconstituted from ^{15}N-labeled NS2B and unlabeled NS3pro likewise indicated the open conformation.[38] In fact, the NS2B segment from Leu86* onward maintained its chemical shifts characteristic of the unfolded peptide even in the complex with bovine pancreatic trypsin inhibitor (BPTI). In contrast, the crystal structure of a slightly different unlinked construct of the Zika virus NS2B-NS3 protease, referred to as bZipro, showed

https://doi.org/10.1021/acssensors.5c00432
ACS Sens. 2025, 10, 3152−3161

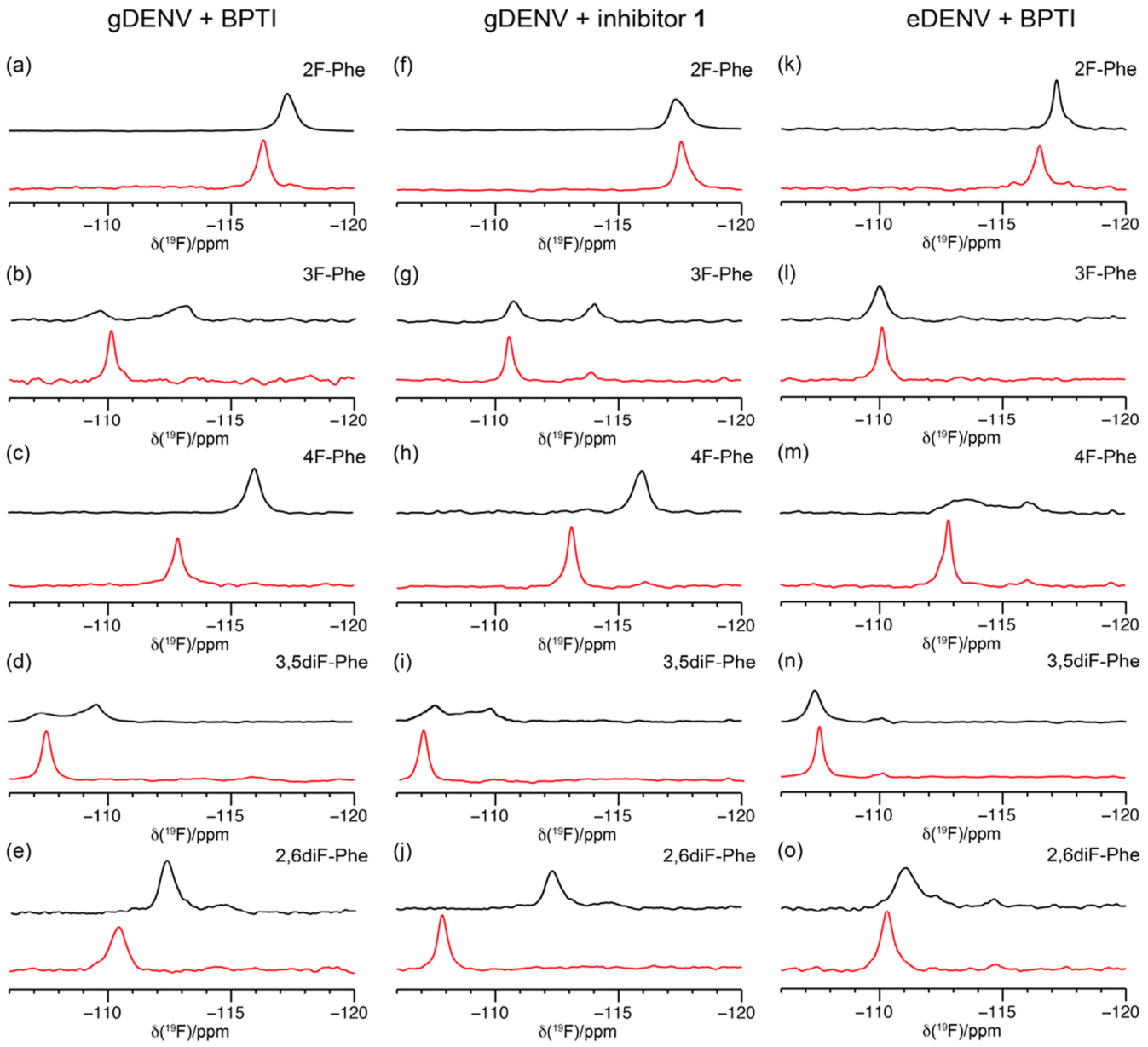

Figure 3. 1D ^{19}F NMR spectra monitoring position 116 in different constructs of the dengue virus (serotype 2) NS2B-NS3 protease. Phe116 in NS3pro was replaced by a fluorinated phenylalanine isomer as indicated. Black and red spectra were recorded in the absence and presence of inhibitor, respectively. Unless mentioned otherwise, the complexes were formed by adding either BPTI in equimolar ratio or the inhibitor **1** in 2-fold excess. All spectra were recorded on a 400 MHz NMR spectrometer and processed with 80 Hz line broadening. The total recording time per spectrum ranged from 80 min to about 3 h depending on the signal intensities. (a−e) Spectra of gDENV, free and in complex with the inhibitor BPTI. (f−j) Spectra of gDENV, free and after reaction with the inhibitor **1**. In (g), each spectrum was recorded overnight to account for the low concentration (0.2 mM) and broad line widths. (k−o) Spectra of eDENV, free and in complex with BPTI.

the canonical closed conformation for the apoprotein (PDB ID 5GPI). NMR analysis of the bZipro construct failed to assign the backbone amide signals of Phe116 and neighboring residues as well as of the NS2B residues 66* to 86* (where the star marks residues of NS2B).[30] The β-hairpin of NS2Bc thus appears conformationally labile in the vicinity of Phe116, which is located at the interface of NS2B and NS3pro (Figure 2).

Phe116 is conserved among the flaviviral NS3 proteases (Figure 2c). It is located at the interface of NS2B and NS3pro but too far from the active site for direct contacts with the substrate (Figure 2). In crystal structures showing the open conformation of the NS2B-NS3 proteases, Phe116 is highly solvent exposed (Table S1). To probe the interaction between NS2Bc and NS3pro, we used the new genetic encoding systems to install the fluorinated phenylalanines of Figure 1 in place of Phe116 and monitored any changes in chemical environment in response to inhibitor binding by ^{19}F NMR.

RESULTS

Selection of Aminoacyl-tRNA Synthetases for Genetic Encoding of Fluorinated Phe Analogues. Initially, a previously established library of mutant pyrrolysyl-tRNA synthetases of the methanogenic archaeon ISO4-G1[19] was screened for enzymes capable of loading the amber suppressor-tRNA from this organism with 2,3,4,5,6-penta-fluorophenyla-

https://doi.org/10.1021/acssensors.5c00432
ACS Sens. 2025, 10, 3152−3161

lanine (F_5-Phe) with the aim of finding G1PylRS mutants with polyspecificity for less highly fluorinated Phe analogues. The protocol of multiple positive (with ncAA) and negative (without ncAA) selection rounds is described in detail in the Supporting Information. Briefly, *E. coli* DH10B cells were cotransformed with pBK-G1RS, which encodes a library of G1PylRS mutants, and pBAD-H6RFP, which is a selection plasmid expressing mCherry red fluorescent protein (RFP) with an amber stop codon following an N-terminal His_6 tag (His_6-TAG-RFP). Successive rounds of fluorescence-activated cell sorting (FACS) were performed, alternating between positive selection in the presence of 1 mM ncAA and negative selection without ncAA. This process progressively enriched the population of cells exhibiting the desired RS activity across fluorophenylalanine variants. The strategy yielded mutants recognizing 3F-Phe, 3,5diF-Phe, and, to a reasonable degree, 2,6diF-Phe, but not 4F-Phe. Therefore, additional library screens were performed with 2F-Phe and 4F-Phe (Figures 1f–h and S2–S5). After the final selection round, colonies displaying high RFP fluorescence were isolated and sequenced, leading to the identification of 13 new G1PylRS mutants (Table S2). In the following applications, the mutant G1-F5F29 was used for the incorporation of 3F-Phe, 2,6diF-Phe, and 3,5diF-Phe. The mutants G1-2FF44 and G1-4FF02 were used for all applications incorporating 2F-Phe and 4F-Phe, respectively.

Production of Flaviviral NS2B-NS3 Proteases with Fluorinated Phe Residues. Samples of gDENV, gZika, eDENV, and eZika were produced with Phe116 replaced by 2F-Phe, 3F-Phe, 4F-Phe, 3,5diF-Phe, or 2,6diF-Phe. The proteins were obtained in good yields, ranging from 5 to 43 mg of purified protein per liter cell culture (Table S3). In general, expression of the constructs containing the covalent Gly_4–Ser–Gly_4 linker delivered higher protein yields than the enzymatically digested constructs, and the DENV proteins were obtained in greater yields than the Zika proteins. Mass spectrometric analysis indicated very low levels of misincorporation arising from decoding of the amber stop codon as Phe or decoding of a Phe codon as a fluorinated phenylalanine (Figures S6–S9). Accepting peaks deviating from the main peak by 16–18 mass units as evidence for misincorporation, the tallest signal indicating misincorporation never exceeded 12% of the main species. The true rate of misincorporation was much lower, however, as suggested by the mass spectra of the NS3pro segment of eZika, which contains only a single Phe codon besides the amber stop codon (Figure S9). In addition, the samples prepared with diF-Phe showed no evidence for the simultaneous loss of two fluorine atoms which would indicate misincorporation of Phe in place of diF-Phe.

^{19}F NMR Spectroscopy of the DENV NS2B-NS3 Protease. We recorded ^{19}F NMR spectra of the gDENV, eDENV, gZika, and eZika constructs in the presence and absence of the inhibitor BPTI and probed the complexes of gDENV and gZika also with the generic serine protease inhibitor *p*-nitrophenyl-*p*-guanidino benzoate (inhibitor **1**; Figure S1). The inhibitor **1** installs the *p*-guanidino benzoate group on the active-site serine residue by trans-esterification, leaving a much smaller footprint than BPTI.

The one-dimensional ^{19}F NMR spectra of gDENV and eDENV prepared with fluorinated phenylalanines in position 116 revealed conformational heterogeneity that was suppressed in the complexes with inhibitor. Most clearly, gDENV produced with 3F-Phe (Figure 3b,g) showed two peaks of similar intensity. A 2D exchange spectrum produced cross-peaks, confirming that the two signals arise from conformational rather than chemical heterogeneity (Figure 4). The peak

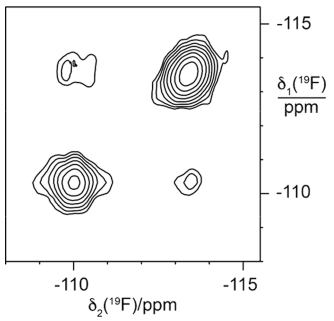

Figure 4. Exchange between different conformations of gDENV with 3F-Phe in position 116. The spectrum was recorded at 25 °C on a 1.3 mM protein solution using the [^{19}F,^{19}F]-NOESY pulse sequence with a mixing time of 200 ms. The total recording time was 18 h. The intensity ratios of the cross-peaks versus the diagonal peaks indicate exchange lifetimes between 1.1 and 1.5 s.

intensities indicated exchange lifetimes between 1 and 1.5 s. The ^{19}F NMR spectra of samples prepared with 3,5diF-Phe similarly showed two peaks, with their relative intensities varying between two different sample preparations (Figure 3d,i). As the intensities of the peaks differ, they must reflect a conformational exchange different from a slow aromatic ring flip. The peaks collapsed into a single peak after the addition of BPTI or inhibitor **1** (Figure 3d,i). The corresponding samples of eDENV did not show the same level of heterogeneity (Figure 3l,n), but also these samples showed significantly narrower signals for the complex with BPTI than the free protein, indicating that conformational heterogeneity is a feature also of free eDENV. The symmetric shape of the NMR signals suggests averaging in the fast exchange regime rather than accidental overlap of different peaks.

The conformational equilibria are influenced by the covalent linker between NS2B and NS3pro, which is present in gDENV but absent from eDENV. In general, the samples made with different versions of fluorinated phenylalanines displayed a narrowing of the ^{19}F NMR signals after the addition of inhibitor despite the concomitant increase in molecular mass of the complexes, indicating suppression of exchange broadening. The only exception was the gDENV sample made with 2,6diF-Phe, where the signal became slightly broader in the complex with BPTI (Figure 3e).

The binding of inhibitors was accompanied by large changes in chemical shifts, exceeding 4 ppm in the case of gDENV with inhibitor **1** (Figure 3j). In view of the distance between the active site and position 116, the effect must be indirect. Importantly, the BPTI complexes of gDENV and eDENV feature practically the same chemical shifts and similar chemical shifts were also observed for the samples of gDENV with inhibitor **1**, suggesting structural conservation of the NS2B-NS3pro interface. Significant differences in chemical shifts between the complexes formed with inhibitor **1** and BPTI were observed only for the samples made with 2F-Phe and 2,6diF-Phe (Figure 3a,f,e,j). As the 2- and 6-positions of the aromatic ring are closer to the backbone than any other ring position, these positions may be more sensitive to small changes in the side chain dihedral angles.

https://doi.org/10.1021/acssensors.5c00432
ACS Sens. 2025, 10, 3152–3161

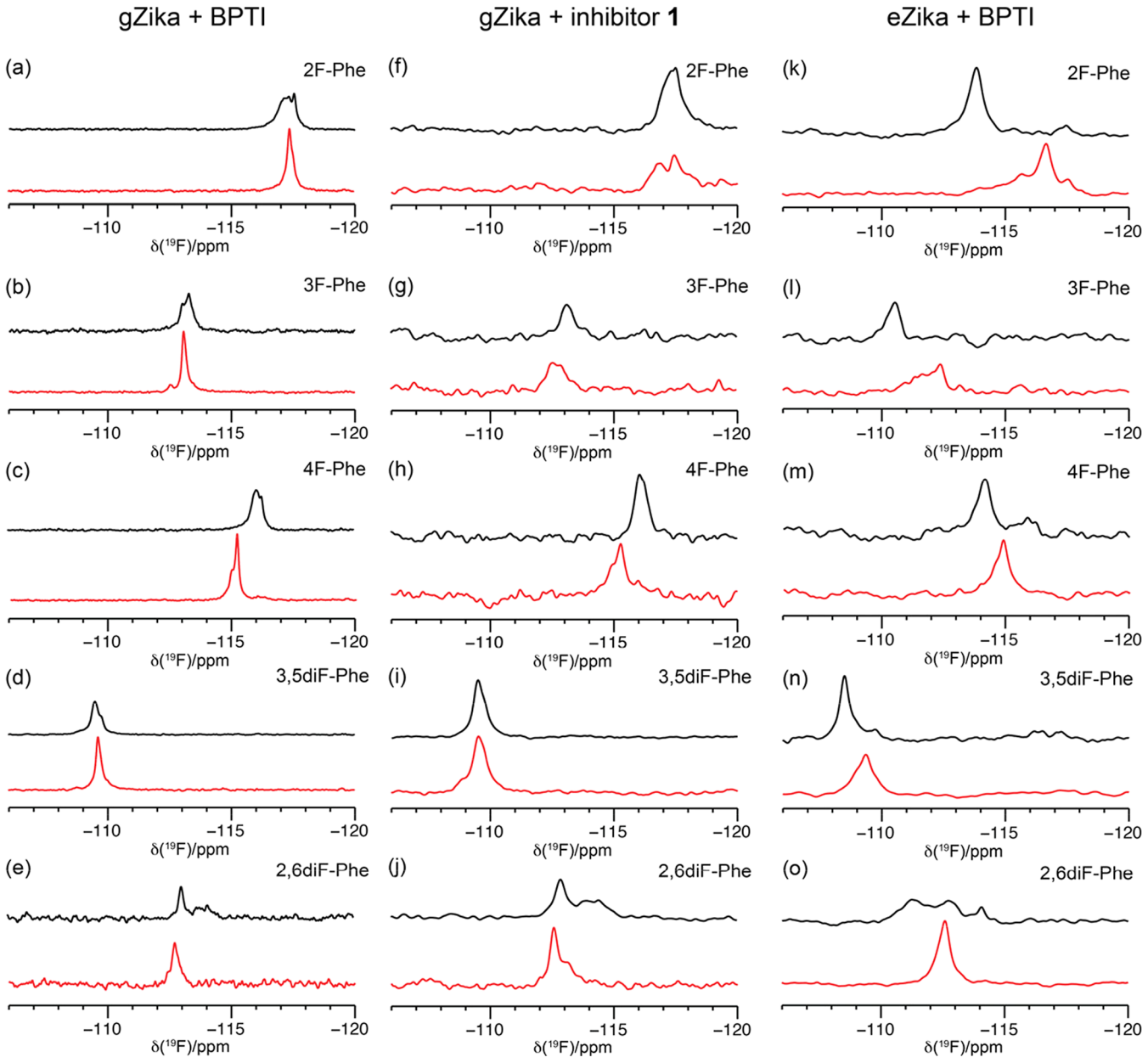

Figure 5. 1D ^{19}F NMR spectra monitoring position 116 in different constructs of the Zika virus NS2B-NS3 protease. Phe116 in NS3pro was replaced by a fluorinated phenylalanine isomer as indicated. Black and red spectra were recorded in the absence and presence of inhibitor, respectively. To form the complexes, BPTI was added in equimolar ratio and the inhibitor **1** in 2-fold excess. The total recording time per spectrum ranged from 15 min (using a cryoprobe on a 600 MHz NMR spectrometer) to 3 h. Unless noted otherwise, all spectra were recorded on the 400 MHz NMR spectrometer. (a−e) Spectra of gZika, free and in complex with the inhibitor BPTI. The FIDs were processed with an exponential window function leading to 30 Hz line broadening. Except for the spectra in (e), the spectra were recorded on the 600 MHz NMR spectrometer. (f−j) Spectra of gZika, free and in complex with the inhibitor **1**, processed with 80 Hz line broadening. (k−o) Spectra of eZika, free and in complex with BPTI added in equimolar ratio, processed with 100 Hz line broadening.

^{19}F NMR Spectroscopy of the Zika Virus NS2B-NS3 Protease. The fluorinated constructs made of the Zika virus NS2B-NS3 protease behaved different from the DENV constructs. Like in DENV, Phe116 of NS3pro is located at the interface to NS2B, but the ^{19}F NMR spectra of gZika and eZika appeared heterogeneous with and without inhibitors and the heterogeneity was more pronounced in the eZika than gZika samples (Figure 5). Furthermore, the presence of inhibitors induced much smaller changes in chemical shifts for gZika. In many of the eZika constructs, the heterogeneity became more pronounced in the complex with BPTI (Figure 5k,l,n). Like with gDENV and eDENV, similar chemical shifts of the complexes indicate similar conformations in the presence of the inhibitors but, in the absence of inhibitors, the chemical shifts differed much more between the gZika and eZika samples than in the case of the eDENV and gDENV samples. This observation is readily explained by the crystal structure of an eZika construct by Phoo et al.,[39] where the Gly_4−Ser−Gly_4 linker was replaced by the recognition site for autocatalytic cleavage (KTGKR; PDB ID 5GJ4). The structure revealed the peptide TGKR to remain bound to the active site after self-cleavage. While the enzyme assumes the closed

https://doi.org/10.1021/acssensors.5c00432
ACS Sens. 2025, 10, 3152−3161

conformation in the crystal, the NMR measurements by Phoo et al. indicated two species of NS2Bc in solution, one showing signal broadening by chemical exchange and the other being highly dynamic in agreement with the dissociated open conformation.[39]

The structural heterogeneity of gZika persisting in the presence of inhibitor **1** is greater than in the complex with BPTI as suggested by greater ranges of chemical shifts, in agreement with the larger interaction surface of BPTI restricting the conformational diversity in the protease. By the same criterion, the heterogeneity in the complexes with BPTI is significantly more pronounced in eZika than gZika, indicating that the covalent linkage between NS2B and NS3pro assists in driving the protease toward a single conformation.

DISCUSSION

Benefit of Selective ^{19}F Labeling by Genetic Encoding. The present work reports systems for the orthogonal genetic encoding of five different versions of fluorinated phenylalanine with excellent selectivity and yields. The successful aminoacyl-tRNA synthetases were selected from a library of mutants derived from the methanogenic archaeon ISO4-G1. The same library has previously been a successful source of selections for a range of different ncAAs.[19−23] The installation of single copies of fluorinated phenylalanine analogues renders the resonance assignment trivial and limits potential perturbations of the protein properties.

In the case of the dengue and Zika virus proteases, the observation of multiple ^{19}F NMR peaks when single resonances were expected is a clear indication of heterogeneity. The heterogeneities must be attributed to different conformations, as mass spectrometry reported high chemical uniformity. The heterogeneities were more clearly reflected by some of the fluorinated phenylalanine isomers than others, with no single isomer being consistently more sensitive. Conceivably, heterogeneities can be hidden by accidental chemical shift degeneracies. Conversely, fluorination may make heterogeneities visible by slowing the exchange between different species. It is thus advantageous that the target proteins can be expressed with different fluorinated phenylalanine isomers using the same, amber-interrupted DNA template.

Evidence and Origin of Conformational Heterogeneities. Conformational heterogeneities in the flaviviral proteases were evidenced not only by a multitude of ^{19}F NMR signals, but also by greater line widths than expected. The line widths of the narrowest ^{19}F NMR signals observed in this work were about 50 Hz, comparable with the narrowest line widths observed for the proteases produced with fluorotryptophans,[22] but most peaks were significantly broader. As we recorded the ^{19}F NMR spectra without ^{1}H decoupling, up to 30 Hz of the line width is due to unresolved aromatic J_{HF} couplings.[40] The omission of ^{1}H decoupling resulted in taller ^{19}F NMR signals by avoiding the transfer of saturation from ^{1}H to ^{19}F spins. Notably, many ^{19}F NMR signals observed in the present work were much broader than 50 Hz, indicating broadening by chemical exchange or unresolved heterogeneity. In the case of the gDENV and eDENV constructs, the heterogeneities were suppressed in the 32 kDa complex with BPTI as evidenced by narrower signals despite the increase in molecular weight. The complex with inhibitor **1** also showed narrower lines.

Exchange broadening in the absence of inhibitors is a common feature of the flaviviral proteases, with the dissociation−association equilibrium of NS2Bc relative to NS3pro presenting a plausible underlying mechanism.[30,39,41,42] Earlier measurements of ^{15}N relaxation rates of backbone amides indicated exchange broadening for some of the backbone nitrogens of the dengue virus protease, including the nitrogen of Phe116.[43] As the binding of inhibitors leads to a tighter association of the β-hairpin of NS2Bc with NS3pro, it is plausible that inhibitor binding also suppresses most of the conformational heterogeneities of the apoprotein.

Available data suggest that the equilibrium between open and closed conformations in the flaviviral NS2B-NS3 proteases results in exchange broadening too fast to detect individual NMR signals for both states.[30,39,41−43] To produce multiple signals with distinctly different chemical shifts, the corresponding conformational states must interconvert on a much slower time scale. Protons on either side of an aromatic ring have been shown to display resolved signals that exchange slowly in proteins restrained by multiple disulfide bonds[44] and the aromatic ring flips may be slowed by fluorination.[45] Conformations populated at different levels as observed in the present work, however, cannot be explained by slow phenyl ring flips. Alternative explanations for slow conformational dynamics could be the cis−trans isomerization of peptide bonds, such as commonly observed for proline residues.[46] In the case of the flaviviral NS2B-NS3 proteases, we previously detected slow exchange processes on the second time scale by ^{19}F NMR of fluorotryptophan residues.[20,22] As the available crystal structures report flips of tryptophan indole rings (Table S1), different side chain orientations of multiple tryptophan residues with variable populations present a plausible alternative explanation for the different species sensed by fluorophenylalanine at position 116.

Notably, the observation of slow conformational exchange is not an artifact of fluorination as several stable conformations in different ratios have been reported previously for the dengue virus NS2B-NS3 protease reconstituted from ^{15}N-labeled NS2B and unlabeled NS3pro. The conformational heterogeneity was not apparent in the linked construct and less prominent or absent in complexes with different peptide inhibitors.[47] Slow conformational exchange between two species has also been reported for a trifluoroacetyl group attached to the Ser75*Cys mutant of the Gly_4−Ser−Gly_4-linked dengue virus NS2B-NS3 protease.[48] The C^{α} atoms of residues 75* and 116 are within 6.5 Å of each other.

The presence of a covalent linkage between NS2B and NS3pro changes the equilibrium between the different conformations. As the unlinked eZika construct showed a broader range of peaks in the complex with BPTI than the gZika construct (Figure 5), the artificial link between NS2B and NS3pro can assist in suppressing the conformational heterogeneities.

Arguably, the peptide linker between the C-terminus of NS2B and the N-terminus of NS3pro imposes only a loose restraint. In the crystal structures of the linked proteases (Figure 2a,b), the last residue of NS2B and first residue of NS3pro observable are separated by ca. 42 Å. As the structures of the dengue and Zika virus proteases miss electron density for the Gly_4−Ser−Gly_4 linker as well as the last 8 residues of NS2B and at least 15 first residues of NS3pro, the combined polypeptide segment of 32 flexible residues covers the required distance easily.

https://doi.org/10.1021/acssensors.5c00432
ACS Sens. 2025, 10, 3152−3161

Effect of BPTI. In contrast to the gDENV and eDENV constructs, evidence for conformational heterogeneity persisted in the case of the gZika and eZika samples in the complexes with inhibitors. There is no cocrystal structure of the Zika virus NS2B-NS3 protease in complex with BPTI. The crystal structure of the dengue virus serotype 3 NS2B-NS3 protease in complex with BPTI (PDB ID 3U1J)[49] shows that the complex does not necessarily stabilize the association of NS2Bc with NS3, as no electron density was observed for NS2B from residue 69* onward. The crystal structures of the BPTI complexes of the NS2B-NS3 proteases from West Nile virus (PDB ID 2IJO)[27] and dengue virus serotype 4 (PDB ID 5YVU and 5YW1)[32] show that the closed conformation can be formed with no clash between NS2Bc and BPTI. In solution, NMR data of the dengue virus serotype 2 NS2B-NS3 protease indicate the closed conformation in the absence of inhibitor regardless of the presence or absence of a Gly_4−Ser−Gly_4-linker[34,35,42,50] and, specifically, also in the complex with BPTI.[36]

CONCLUSION

New genetic encoding systems for high-yielding site-selective installation of five different fluorinated phenylalanine analogues afford the targeted installation of single fluorinated residues. Aided by the exceptional chemical shift dispersion of ^{19}F nuclei, the resulting ^{19}F NMR spectra enable the robust detection and quantification of minor conformational species as well as measurements of rates of interconversion. In the case of the Zika virus NS2B-NS3 protease, the ^{19}F NMR spectra revealed a greater conformational diversity than detected previously by high-field ^{1}H NMR spectroscopy. Even for protein complexes with a molecular weight exceeding 30 kDa, the fluorinated amino acid probes can be monitored by ^{19}F NMR using conventional 400 MHz NMR spectrometers. In view of the ease, with which the genetic encoding systems deliver selectively labeled proteins, we predict that they will become popular tools for the analysis of proteins and protein interactions in solution and in the solid state, including protein-observed ^{19}F NMR for ligand screening,[51] in-cell NMR,[52] and solid-state protein structure determination.[53] Finally, the genetic encoding systems pave the way for protein engineers to stabilize protein folds by installing multiple fluorophenylalanine residues.[54] To encourage the adoption of this uniquely powerful technology, the requisite plasmids have been deposited at Addgene plasmid repository (Watertown, MA, USA; plasmid nos. 232253, 232254, and 232255).

ASSOCIATED CONTENT

Supporting Information

The Supporting Information is available free of charge at https://pubs.acs.org/doi/10.1021/acssensors.5c00432.

Experimental procedures describing (a) materials, (b) selection of functional G1PylRS enzymes recognizing fluorinated phenylalanines, (c) in vivo protein expression and purification, (d) intact protein mass spectrometry, and (e) NMR spectroscopy; chemical structure of inhibitor **1**; FACS experiments for selecting functional G1PylRS enzymes; mass spectra; analysis of crystal structures; protein yields amino acid sequences of proteins (PDF)

AUTHOR INFORMATION

Corresponding Authors

Thomas Huber − *Research School of Chemistry, Australian National University, Canberra, Australian Capital Territory 2601, Australia;* orcid.org/0000-0002-3680-8699; Email: t.huber@anu.edu.au

Gottfried Otting − *ARC Centre of Excellence for Innovations in Peptide & Protein Science, Research School of Chemistry, Australian National University, Canberra, Australian Capital Territory 2601, Australia;* orcid.org/0000-0002-0563-0146; Email: gottfried.otting@anu.edu.au

Authors

Haocheng Qianzhu − *Research School of Chemistry, Australian National University, Canberra, Australian Capital Territory 2601, Australia;* orcid.org/0000-0002-7546-4411

Yi Jiun Tan − *ARC Centre of Excellence for Innovations in Peptide & Protein Science, Research School of Chemistry, Australian National University, Canberra, Australian Capital Territory 2601, Australia*

Elwy H. Abdelkader − *ARC Centre of Excellence for Innovations in Peptide & Protein Science, Research School of Chemistry, Australian National University, Canberra, Australian Capital Territory 2601, Australia;* orcid.org/0000-0002-5388-3949

Complete contact information is available at: https://pubs.acs.org/10.1021/acssensors.5c00432

Author Contributions

[§]H.Q. and Y.J.T. contributed equally to this work.

Notes

The authors declare no competing financial interest.

ACKNOWLEDGMENTS

The authors thank Dr. Harpreet Vohra and Michael Devoy at the John Curtin School of Medical Research, Australian National University, for technical support on FACS experiments. Financial support by the Australian Research Council, including the Centre of Excellence for Innovations in Peptide and Protein Science (CE200100012) and a Discovery Project (DP230100079) is gratefully acknowledged.

REFERENCES

(1) Gamcsik, M. P.; Gerig, J. T. NMR studies of fluorophenylalanine-containing carbonic anhydrase. *FEBS Lett.* **1986**, *196*, 71−74.

(2) Li, H.; Frieden, C. NMR studies of 4-^{19}F-phenylalanine-labeled intestinal fatty acid binding protein: evidence for conformational heterogeneity in the native state. *Biochemistry* **2005**, *44*, 2369−2377.

(3) Welte, H.; Zhou, T.; Mihajlenko, X.; Mayans, O.; Kovermann, M. What does fluorine do to a protein? Thermodynamic, and highly-resolved structural insights into fluorine-labelled variants of the cold shock protein. *Sci. Rep.* **2020**, *10*, 2640.

(4) Tan, Y. J.; Abdelkader, E. H.; Tarcoveanu, E.; Maleckis, A.; Nitsche, C.; Otting, G. (2*S*,4*S*)-5-Fluoroleucine, (2*S*,4*R*)-5-fluoroleucine, and 5,5′-difluoroleucine in *E. coli* PpiB: protein production, ^{19}F NMR, and ligand sensing enhanced by the γ-gauche effect. *Biochemistry* **2024**, *63*, 1376−1387.

(5) Frkic, R. L.; Tan, Y. J.; Abdelkader, E. H.; Maleckis, A.; Tarcoveanu, E.; Nitsche, C.; Otting, G.; Jackson, C. J. Conformational preferences of the non-canonical amino acids (2*S*,4*S*)-5-fluoroleucine, (2*S*,4*R*)-5-fluoroleucine, and 5,5′-difluoroleucine in a protein. *Biochemistry* **2024**, *63*, 1388−1394.

(6) Frkic, R. L.; Tan, Y. J.; Maleckis, A.; Chilton, N. F.; Otting, G.; Jackson, C. J. 1.3 Å crystal structure of *E. coli* peptidyl−prolyl isomerase B with uniform substitution of valine by (2*S*,3*S*)-4-fluorovaline reveals structure conservation and multiple staggered rotamers of CH_2F groups. *Biochemistry* **2024**, *63*, 2602−2608.
(7) Kitevski-LeBlanc, J. L.; Evanics, F.; Scott Prosser, R. Optimizing ^{19}F NMR protein spectroscopy by fractional bio-synthetic labeling. *J. Biomol. NMR* **2010**, *48*, 113−121.
(8) Boeszoermenyi, A.; Ogórek, B.; Jain, A.; Arthanari, H.; Wagner, G. The precious fluorine on the ring: fluorine NMR for biological systems. *J. Biomol. NMR* **2020**, *74*, 365−379.
(9) Toscano, G.; Holzinger, J.; Nagl, B.; Kontaxis, G.; Kählig, H.; Konrat, R.; Lichtenecker, R. J. Decorating phenylalanine side-chains with triple labeled $^{13}C/^{19}F/^{2}H$ isotope patterns. *J. Biomol. NMR* **2024**, *78*, 139−147.
(10) Sun, Z.-Y.; Truong, H.-T. N.; Pratt, E. A.; Sutherland, D. C.; Kulig, C. E.; Homer, R. J.; Groetsch, S. M.; Hsue, P. Y.; Ho, C. A ^{19}F-NMR study of the membrane-binding region of D-lactate dehydrogenase of *Escherichia coli*. *Protein Sci.* **1993**, *2*, 1938−1947.
(11) Gerig, J. T. Fluorine NMR of proteins. *Prog. Nucl. Magn. Reson. Spectrosc.* **1994**, *26*, 293−370.
(12) Pless, S. A.; Millen, K. S.; Hanek, A. P.; Lynch, J. W.; Lester, H. A.; Lummis, S. C. R.; Dougherty, D. A. A cation-π interaction in the binding site of the glycine receptor is mediated by a phenylalanine residue. *J. Neurosci.* **2008**, *28*, 10937−10942.
(13) Furter, R. Expansion of the genetic code: site-directed *p*-fluorophenylalanine incorporation in *Escherichia coli*. *Protein Sci.* **1998**, *7*, 419−426.
(14) Young, D. D.; Young, T. S.; Jahnz, M.; Ahmad, I.; Spraggon, G.; Schultz, P. G. An evolved aminoacyl-tRNA synthetase with atypical polysubstrate specificity. *Biochemistry* **2011**, *50*, 1894−1900.
(15) Wang, Y.-S.; Fang, X.; Chen, H.-Y.; Wu, B.; Wang, Z. U.; Hilty, C.; Liu, W. R. Genetic incorporation of twelve *meta*-substituted phenylalanine derivatives using a single pyrrolysyl-tRNA synthetase mutant. *ACS Chem. Biol.* **2013**, *8*, 405−415.
(16) Ko, J.-h.; Wang, Y.-S.; Nakamura, A.; Guo, L.-T.; Söll, D.; Umehara, T. Pyrrolysyl-tRNA synthetase variants reveal ancestral aminoacylation function. *FEBS Lett.* **2013**, *587*, 3243−3248.
(17) Lee, Y.-J.; Schmidt, M. J.; Tharp, J. M.; Weber, A.; Koenig, A. L.; Zheng, H.; Gao, J.; Waters, M. L.; Summerer, D.; Liu, W. R. Genetically encoded fluorophenylalanines enable insights into the recognition of lysine trimethylation by an epigenetic reader. *Chem. Commun.* **2016**, *52*, 12606−12609.
(18) Galles, G. D.; Infield, D. T.; Clark, C. J.; Hemshorn, M. L.; Manikandan, S.; Fazan, F.; Rasouli, A.; Tajkhorshid, E.; Galpin, J. D.; Cooley, R. B.; Mehl, R. A.; Ahern, C. A. Tuning phenylalanine fluorination to assess aromatic contributions to protein function and stability in cells. *Nat. Commun.* **2023**, *14*, 59.
(19) Abdelkader, E. H.; Qianzhu, H.; George, J.; Frkic, R. L.; Jackson, C. J.; Nitsche, C.; Otting, G.; Huber, T. Genetic encoding of cyanopyridylalanine for in-cell protein macrocyclization by the nitrile−aminothiol click reaction. *Angew. Chem., Int. Ed.* **2022**, *61*, No. e202114154.
(20) Qianzhu, H.; Abdelkader, E. H.; Herath, I. D.; Otting, G.; Huber, T. Site-specific incorporation of 7-fluoro-L-tryptophan into proteins by genetic encoding to monitor ligand binding by ^{19}F NMR spectroscopy. *ACS Sens.* **2022**, *7*, 44−49.
(21) Abdelkader, E. H.; Qianzhu, H.; Huber, T.; Otting, G. Genetic encoding of 7-aza-L-tryptophan: Isoelectronic substitution of a single CH-group in a protein for a nitrogen atom for site-selective isotope labeling. *ACS Sens.* **2023**, *8*, 4402−4406.
(22) Qianzhu, H.; Abdelkader, E. H.; Otting, G.; Huber, T. Genetic encoding of fluoro-L-tryptophans for site-specific detection of conformational heterogeneity in proteins by NMR spectroscopy. *J. Am. Chem. Soc.* **2024**, *146*, 13641−13650.
(23) Qianzhu, H.; Abdelkader, E. H.; Welegedara, A. P.; Habel, E.; Paul, N.; Frkic, R. L.; Jackson, C. J.; Huber, T.; Otting, G. Rendering proteins fluorescent inconspicuously: genetically encoded 4-cyano-tryptophan conserves their structure and enables the detection of ligand binding sites. *Angew. Chem., Int. Ed.* **2024**, *64*, No. e202421000.
(24) Kozlowski, L. P. Proteome-pI 2.0: proteome isoelectric point database update. *Nucleic Acids Res.* **2022**, *50*, D1535−D1540.
(25) Samrat, S. K.; Xu, J.; Li, Z.; Zhou, J.; Li, H. Antiviral agents against flavivirus protease: prospect and future direction. *Pathogens* **2022**, *11*, 293.
(26) Erbel, P.; Schiering, N.; D'Arcy, A.; Renatus, M.; Kroemer, M.; Lim, S. P.; Yin, Z.; Keller, T. H.; Vasudevan, S. G.; Hommel, U. Structural basis for the activation of flaviviral NS3 proteases from dengue and West Nile virus. *Nat. Struct. Mol. Biol.* **2006**, *13*, 372−373.
(27) Aleshin, A. E.; Shiryaev, S. A.; Strongin, A. Y.; Liddington, R. C. Structural evidence for regulation and specificity of flaviviral proteases and evolution of the *Flaviviridae* fold. *Protein Sci.* **2007**, *16*, 795−806.
(28) Yildiz, M.; Ghosh, S.; Bell, J. A.; Sherman, W.; Hardy, J. A. Allosteric inhibition of the NS2B-NS3 protease from dengue virus. *ACS Chem. Biol.* **2013**, *8*, 2744−2752.
(29) Lei, J.; Hansen, G.; Nitsche, C.; Klein, C. D.; Zhang, L.; Hilgenfeld, R. Crystal structure of Zika virus NS2B-NS3 protease in complex with a boronate inhibitor. *Science* **2016**, *353*, 503−505.
(30) Zhang, Z.; Li, Y.; Loh, Y. R.; Phoo, W. W.; Hung, A. W.; Kang, C.; Luo, D. Crystal structure of unlinked NS2B-NS3 protease from Zika virus. *Science* **2016**, *354*, 1597−1600.
(31) Chen, X.; Yang, K.; Wu, C.; Chen, C.; Hu, C.; Buzovetsky, O.; Wang, Z.; Ji, X.; Xiong, Y.; Yang, H. Mechanisms of activation and inhibition of Zika virus NS2B-NS3 protease. *Cell Res.* **2016**, *26*, 1260−1263.
(32) Phoo, W. W.; El Sahili, A.; Zhang, Z.; Chen, M. W.; Liew, C. W.; Lescar, J.; Vasudevan, S. G.; Luo, D. Crystal structures of full length DENV4 NS2B-NS3 reveal the dynamic interaction between NS2B and NS3. *Antiviral Res.* **2020**, *182*, 104900.
(33) Leung, D.; Schroder, K.; White, H.; Fang, N.-X.; Stoermer, M. J.; Abbenante, G.; Martin, J. L.; Young, P. R.; Fairlie, D. P. Activity of recombinant dengue 2 virus NS3 protease in the presence of a truncated NS2B co-factor, small peptide substrates, and inhibitors. *J. Biol. Chem.* **2001**, *276*, 45762−45771.
(34) Kim, Y. M.; Gayen, S.; Kang, C.; Joy, J.; Huang, Q.; Chen, A. S.; Wee, J. L. K.; Ang, M. J. Y.; Lim, H. A.; Hung, A. W.; Li, R.; Noble, C. G.; Lee, L. T.; Yip, A.; Wang, Q.-Y.; Chia, C. S. B.; Hill, J.; Shi, P.-Y.; Keller, T. H. NMR analysis of a novel enzymatically active unlinked dengue NS2B-NS3 protease complex. *J. Biol. Chem.* **2013**, *288*, 12891−12900.
(35) de la Cruz, L.; Chen, W.-N.; Graham, B.; Otting, G. Binding mode of the activity-modulating C-terminal segment of NS2B to NS3 in the dengue virus NS2B−NS3 protease. *FEBS J.* **2014**, *281*, 1517−1533.
(36) Chen, W.-N.; Loscha, K. V.; Nitsche, C.; Graham, B.; Otting, G. The dengue virus NS2B-NS3 protease retains the closed conformation in the complex with BPTI. *FEBS Lett.* **2014**, *588*, 2206−2211.
(37) Mahawaththa, M. C.; Pearce, B. J. G.; Szabo, M.; Graham, B.; Klein, C. D.; Nitsche, C.; Otting, G. Solution conformations of a linked construct of the Zika virus NS2B-NS3 protease. *Antiviral Res.* **2017**, *142*, 141−147.
(38) Roy, A.; Lim, L.; Srivastava, S.; Lu, Y.; Song, J. Solution conformations of Zika NS2B-NS3pro and its inhibition by natural products from edible plants. *PLoS One* **2017**, *12*, No. e0180632.
(39) Phoo, W. W.; Li, Y.; Zhang, Z.; Lee, M. Y.; Loh, Y. R.; Tan, Y. B.; Ng, E. Y.; Lescar, J.; Kang, C.; Luo, D. Structure of the NS2B-NS3 protease from Zika virus after self-cleavage. *Nat. Commun.* **2016**, *7*, 13410.
(40) Emsley, J. W.; Phillips, L.; Wray, V. Flourine coupling constants. *Prog. Nucl. Magn. Reson. Spectrosc.* **1976**, *10*, 83−752.
(41) Su, X.-C.; Ozawa, K.; Qi, R.; Vasudevan, S. G.; Lim, S. P.; Otting, G. NMR analysis of the dynamic exchange of the NS2B cofactor between open and closed conformations of the West Nile virus NS2B-NS3 protease. *PLoS Neglected Trop. Dis.* **2009**, *3*, No. e561.

https://doi.org/10.1021/acssensors.5c00432
ACS Sens. 2025, 10, 3152−3161

(42) de la Cruz, L.; Nguyen, T. H. D.; Ozawa, K.; Shin, J.; Graham, B.; Huber, T.; Otting, G. Binding of low-molecular weight inhibitors promotes large conformational changes in the dengue virus NS2B-NS3 protease: fold analysis by pseudocontact shifts. *J. Am. Chem. Soc.* **2011**, *133*, 19205−19215.
(43) Agback, T.; Lesovoy, D.; Han, X.; Lomzov, A.; Sun, R.; Sandalova, T.; Orekhov, V. Y.; Achour, A.; Agback, P. Combined NMR and molecular dynamics conformational filter identifies unambiguously dynamic ensembles of Dengue protease NS2B/NS3pro. *Commun. Biol.* **2023**, *6*, 1193.
(44) Wagner, G.; Brühwiler, D.; Wüthrich, K. Reinvestigation of the aromatic side-chains in the basic pancreatic trypsin inhibitor by heteronuclear two-dimensional nuclear magnetic resonance. *J. Mol. Biol.* **1987**, *196*, 227−231.
(45) Lian, C.; Le, H.; Montez, B.; Patterson, J.; Harrell, S.; Laws, D.; Matsumura, I.; Pearson, J.; Oldfield, E. Fluorine-19 nuclear magnetic resonance spectroscopic study of fluorophenylalanine- and fluorotryptophan-labeled avian egg white lysozymes. *Biochemistry* **1994**, *33*, 5238−5245.
(46) Yonezawa, Y.; Nakata, K.; Sakakura, K.; Takada, T.; Nakamura, H. Intra- and intermolecular interaction inducing pyramidalization on both sides of a proline dipeptide during isomerization: an ab initio QM/MM molecule dynamics simulation study in explicit water. *J. Am. Chem. Soc.* **2009**, *131*, 4535−4540.
(47) Woestenenk, E.; Agback, P.; Unnerståle, S.; Henderson, I.; Agback, T. Co-refolding of a functional complex of Dengue NS3 protease and NS2B co-factor domain and backbone resonance assignment by solution NMR. *Protein Expression Purif.* **2017**, *140*, 16−27.
(48) Zhu, L.; Yang, J.; Li, H.; Sun, H.; Liu, J.; Wang, J. Conformational change study of dengue virus NS2B-NS3 protease using ^{19}F NMR spectroscopy. *Biochem. Biophys. Res. Commun.* **2015**, *461*, 677−680.
(49) Noble, C. G.; Seh, C. C.; Chao, A. T.; Shi, P. Y. Ligand-bound structures of the dengue virus protease reveal the active conformation. *J. Virol.* **2012**, *86*, 438−446.
(50) Li, H.; Zhu, L.; Hou, S.; Yang, J.; Wang, J.; Liu, J. An inhibition model of BPTI to unlinked dengue virus NS2B-NS3 protease. *FEBS Lett.* **2014**, *588*, 2794−2799.
(51) Arntson, K. E.; Pomerantz, W. C. K. Protein-observed fluorine NMR: A bioorthogonal approach for small molecule discovery. *J. Med. Chem.* **2016**, *59*, 5158−5171.
(52) Ye, Y.; Liu, X.; Zhang, Z.; Wu, Q.; Jiang, B.; Jiang, L.; Zhang, X.; Liu, M.; Pielak, G. J.; Li, C. ^{19}F NMR spectroscopy as a probe of cytoplasmic viscosity and weak protein interactions in living cells. *Chem.—Eur. J.* **2013**, *19*, 12705−12710.
(53) Shcherbakov, A. A.; Mandala, V. S.; Hong, M. High-sensitivity detection of nanometer ^{1}H−^{19}F distances for protein structure determination by ^{1}H-detected fast MAS NMR. *J. Phys. Chem. B* **2019**, *123*, 4387−4391.
(54) Hsu, W.-L.; Shih, T.-C.; Horng, J.-C. Folding stability modulation of the villin headpiece helical subdomain by 4-fluorophenylalanine and 4-methylphenylalanine. *Biopolymers* **2015**, *103*, 627−637.

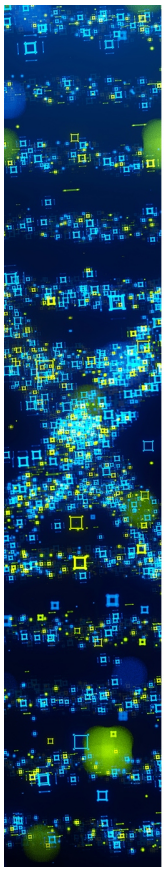
CAS BIOFINDER DISCOVERY PLATFORM™
STOP DIGGING THROUGH DATA —START MAKING DISCOVERIES
CAS BioFinder helps you find the right biological insights in seconds
Start your search
CAS
A division of the American Chemical Society

https://doi.org/10.1021/acssensors.5c00432
ACS Sens. 2025, 10, 3152−3161